

# Synthesis and Characterization of $\text{LaNi}_x\text{Co}_{1-x}\text{O}_3$ Perovskites via Complex Precursor Methods

Grace Rafaela Oliveira Silva<sup>1,2</sup>, José Carlos Santos<sup>1</sup>, Danielle M. H. Martinelli<sup>3</sup>, Anne Michelle Garrido Pedrosa<sup>1\*</sup>, Marcelo José Barros de Souza<sup>2</sup>, Dulce Maria Araujo Melo<sup>3</sup>

<sup>1</sup>Departamento de Química, Universidade Federal de Sergipe, São Cristóvão, Brazil; <sup>2</sup>Departamento de Engenharia Química, Universidade Federal de Sergipe, São Cristóvão, Brazil; <sup>3</sup>Universidade Federal do Rio Grande do Norte, Departamento de Química, Natal, Brazil.

Email: [annemgp@yahoo.com](mailto:annemgp@yahoo.com)

Received February 7<sup>th</sup>, 2010; revised April 20<sup>th</sup>, 2010; accepted April 22<sup>nd</sup>, 2010.

## ABSTRACT

*This work presents a study on the synthesis of  $\text{LaNi}_x\text{Co}_{1-x}\text{O}_3$  perovskites via complex precursor methods. Perovskite oxides with the composition  $\text{LaNi}_x\text{Co}_{1-x}\text{O}_3$  were synthesized by chelating precursor and polymeric precursor methods using nickel and/or cobalt nitrates, lanthanum nitrate, ethylene glycol, citric acid, and EDTA as starting source. The obtained perovskite were characterized by thermogravimetric analysis, infrared spectroscopy, X-ray diffraction and the morphology of the samples were investigated by  $\text{N}_2$  adsorption experiments and average medium particle size. TG curves and FTIR spectra were particularly useful in establishing of the optimal calcination temperature of the precursor powders. X-ray diffraction patterns revealed the formation of the perovskite structure in all samples prepared by both synthesis method and after calcinations at 700°C. The results showed that the preparation method resulted in oxides with the intended structure. The specific surface area values were influenced by preparation method.*

**Keywords:**  $\text{LaNi}_x\text{Co}_{1-x}\text{O}_3$  Perovskites, EDTA, Complex Precursor Methods

## 1. Introduction

The perovskite-type oxides have received much attention in the last years because of their potential application as electrode materials in solid oxide fuel cells, as gas sensors, in various interesting reactions, such as in the steam reforming and in the dried reforming of hydrocarbons, in the catalytic combustion and as oxygen-permeable membranes [1-4]. Such materials have various advantages as: wide variety of composition and constituent elements keeping essentially the basic structure unchanged, bulk structure can be characterized well, their surface can be fairly well estimated taking advantage of this well-defined bulk structure, their valency, stoichiometry and vacancy can be varied widely and huge information on physical and solid-state chemical properties has been accumulated [5-7].

A perovskite-type mixed oxide can be described by the general stoichiometric formula  $\text{ABO}_3$ , where A represents a lanthanide or alkaline earth ion and B a transition metal ion trivalent, generally. The perovskite lattice can accommodate multiple cationic substitutions with only small changes since the value of the structure factor ( $t$ ) is between 0.75 and 1 [8]. In this structure, the properties are

mainly determined by the occupancy of B sites, which usually are partially substituted [8-9].

The properties studied for the different perovskite oxides are potentially influenced by the synthesis method, calcination conditions (temperature, time and atmosphere) and substitutions of A and/or B sites [5-7,10]. The effects of these variables have been studied in order to optimize the performance of the material. The properties of perovskite can be enhanced by the substitution of lanthanum by strontium [11-12] or even cerium [13-14]. However, the catalytic activity of perovskites is mainly determined by the type of metal that occupies the B sites and the partial substitution of those sites [8-9,15-17]. Substitutions in the A and/or B sites can be cause the formation of defects that modify the catalytic properties [15,18].

Several methods have been used so far to prepare these materials, such as freeze-drying, spray-drying, co-precipitation, hydrothermal synthesis and combustion of metal-organic precursors [19-21]. Chelating ligands which contain carboxylate groups or carboxylate and aliphatic amine groups are essential in the water-soluble complex precursor synthesis route. Citric acid (containing carboxylate groups) or ethylenediaminetetraacetic acid (ED-

TA) (containing carboxylate and aliphatic amine groups) were often used before in the synthesis of perovskite oxide. In this work,  $\text{LaNi}_x\text{Co}_{1-x}\text{O}_3$  perovskites were synthesized by polymeric precursor method (PP) and chelating precursor method (PQ). The effects of chelating agents on the synthesis procedure and the evolution of crystalline phase have been investigated. These methods normally involve three sequential steps: preparing an aqueous solution of chelated complexes, concentrating the solution to form a gel, and pyrolyzing the gel to produce an amorphous oxide powder.

## 2. Experimental

### *Synthesis of the perovskites by chelating precursors (PQ) method:*

$\text{LaMO}_3$  ( $M = \text{Ni}$  or  $\text{Co}$ ) perovskites were synthesized by chelating precursors method using lanthanum, nickel and cobalt nitrates, citric acid and using ethylenediamine-tetraacetic acid (EDTA) as chelating agent. Citrate aqueous solution were prepared from stoichiometric amounts of  $\text{La}(\text{NO}_3)_3 \cdot 6\text{H}_2\text{O}$ ,  $\text{Ni}(\text{NO}_3)_2 \cdot 6\text{H}_2\text{O}$  and  $\text{Co}(\text{NO}_3)_2 \cdot 6\text{H}_2\text{O}$  and citric acid in 1:2 molar ratio (metal: citric acid). EDTA aqueous solution was prepared separately by continuous stirring until complete dissolution. This solution was added slowly to citrate solutions under constant mixing for 15 minutes with  $\text{pH} \approx 9$ . With addition of EDTA solution the resultant color was changed. Such solutions were added to obtain a precursor solution in which M-EDTA molar ratio was 1:1 ( $M = \text{metal} = \text{La}$  and  $\text{Ni}$  or  $\text{Co}$ ). After achieving complete dissolution, the resultant solution was dried in a stove at  $160^\circ\text{C}$  for 3 h. After the precursor solution was maintained under vacuum producing a viscous mass. The resultant material was heated treated at  $220^\circ\text{C}$  for 30 minutes at a heating rate of  $10^\circ\text{C}/\text{min}$ . The sponge-like green resin was formed. This solid resin precursor was calcined at  $700^\circ\text{C}$  for 8 hours at a heating rate of  $10^\circ\text{C}/\text{min}$ .

### *Synthesis of the perovskites by polymeric precursors (PP) method:*

Perovskite oxides with the composition  $\text{LaNi}_x\text{Co}_{1-x}\text{O}_3$  ( $0.4 \leq x \leq 0.6$ ; or  $x = 1$ ) were synthesized using the precursor polymeric method [22]. Solutions of cobalt citrate and nickel citrate were prepared from  $\text{Co}(\text{NO}_3)_2 \cdot 6\text{H}_2\text{O}$ ,  $\text{Ni}(\text{NO}_3)_2 \cdot 6\text{H}_2\text{O}$  and citric acid-AC (molar ratio of 2.5) under constant stirring at  $70^\circ\text{C}$  for 30 min. Stoichiometric contents of  $\text{La}(\text{NO}_3)_3 \cdot 6\text{H}_2\text{O}$  solid were mixed with nickel citrate solutions at  $70^\circ\text{C}$  for 20 min. The cobalt citrate solution was then added under similar conditions. After complete mixing, the temperature was slowly increased to  $90^\circ\text{C}$ , at which point ethylene glycol was added in the ratio of 60:40 (citric acid: ethylene glycol). The resulting solution was maintained at that temperature for 2 h under constant magnetic stirring. A gel was then formed and subsequently heat-treated at  $300^\circ\text{C}$  for 2 h resulting in the precursor powders. These materials were calcined at

$700^\circ\text{C}$  for 4 h at a heating rate of  $10^\circ\text{C}/\text{min}$ .

### *Characterizations of the perovskites*

Thermogravimetric analyses of the precursor powders were carried out on a Perkin Elmer TGA-7 instrument at a heating rate of  $5^\circ\text{C}/\text{min}$  under air flowing at a rate of  $50 \text{ cm}^3/\text{min}$ . The eventual presence of organic material after calcination was determined by infrared spectroscopy within the interval from  $4000$  to  $500 \text{ cm}^{-1}$  in an ABB BOMER instrument model MB104 using KBr pellets. X-ray diffraction patterns were obtained from a Shimadzu XRD-6000 diffractometer by scanning the angular range  $10^\circ \leq 2\theta \leq 90^\circ$  using  $\text{CuK}_\alpha$  radiation ( $\lambda = 1.5418 \text{ \AA}$ ). The specific surface area of the powders was measured by nitrogen adsorption on a NOVA 2000 system. The specific surface area was estimated by Brunauer, Emmet and Teller (BET) method. The microstructure of the powders was revealed observing Au-coated samples under a Philips ESEM-XL30 scanning electron microscopy set at the high-vacuum mode.

## 3. Results and Discussion

Thermal analysis has been found to yield information on the decomposition temperatures of oxides as also about its thermal stability [23]. Thermogravimetric curves of  $\text{LaMO}_3$  ( $\text{Ni}$  or  $\text{Co}$ ) heated treated at  $220^\circ\text{C}$  and prepared by PQ method are shown in **Figure 1(a)**. TG curves showed an initial mass loss of about 21% in the temperature range of  $30$ - $315^\circ\text{C}$  that is attributed to water loss, EDTA initial decomposition and citrate/nitrate decompositions. A second loss weight of 39% can be observed in the range  $315$ - $540^\circ\text{C}$  which is due EDTA decomposition given perovskite oxide, sodium carbonate and sodium oxide. For comparison, TG/DTG curves for EDTA pure are shown in the **Figure 1(b)**. The curves shown typically four regions of mass loss in the temperature range studied. EDTA thermo decomposition starting at  $30^\circ\text{C}$  and following until  $750^\circ\text{C}$ . In the temperature range of  $750$ - $850^\circ\text{C}$  there is formation of a stable product that was attributed to sodium carbonate and/or sodium oxide. The residue of pure EDTA decomposition at  $773^\circ\text{C}$  for 2 hours was characterized by XRD (Figure not shown) and was observed the formation of predominantly sodium carbonate. It can be seen from Figure 1a that the decomposition of EDTA molecules in the  $\text{LaMO}_3$  ( $\text{Ni}$  or  $\text{Co}$ ) heated treated at  $220^\circ\text{C}$  and prepared by PQ method starts at different temperature than in EDTA pure. TG/DTG curves of the EDTA residue obtained by calcinations at  $773^\circ\text{C}$  for 2 hours (Figure not shown) showed an initial mass loss of about 9% in the temperature range of  $80$ - $108^\circ\text{C}$  that was attributed to water loss. A second loss weight of about 90% in the temperature range of  $860$ - $1200^\circ\text{C}$  was attributed to decomposition of sodium carbonate, revealing the predominant presence of this material in the temperature range of  $750$  at  $860^\circ\text{C}$ . For the samples heated treated at  $220^\circ\text{C}$ , the complexation of nickel or cobalt and lantha-

num ions with EDTA ligand influence on the EDTA interactions and consequently in their decomposition temperature. Therefore, in these samples the temperature required for EDTA decomposition is at  $540^\circ\text{C}$  (**Figure 1(a)**) and the residue is composed perovskite oxide, sodium carbonate and sodium oxide. A loss mass observe at temperature up to  $850^\circ\text{C}$  is due of sodium carbonate decomposition.

TG curves of  $\text{LaNi}_x\text{Co}_{1-x}\text{O}_3$  ( $0.4 \leq x \leq 0.6$ ;  $x = 1$ ) heated treated at  $300^\circ\text{C}$  and prepared by PP method are shown in **Figure 1c**. The first step took place at about  $30^\circ\text{C}$  with the onset of decomposition of the residual material synthesis and following until  $350^\circ\text{C}$ . Full decomposition of residual material occurred between  $350$  and  $650^\circ\text{C}$ , followed by perovskite oxide formation.

For the samples  $\text{LaNi}_x\text{Co}_{1-x}\text{O}_3$  ( $0.4 \leq x \leq 0.6$ ;  $x = 1$ ) calcined at  $700^\circ\text{C}$  and prepared by PP method, TG curves not shown loss mass in the range of  $30$ - $900^\circ\text{C}$ .

For the other hand, for the samples  $\text{LaMO}_3$  (Ni or Co), calcined at  $700^\circ\text{C}$  and prepared by PQ method (**Figure not shown**), TG curves showed that the thermal decomposition took place in two steps stabilizing at temperatures high than  $1100^\circ\text{C}$ . The mass loss observed between  $30$ - $140^\circ\text{C}$  was attributed to several simultaneous decomposition reactions of the residual material of the synthesis process. The samples still showed another decomposition step above  $850^\circ\text{C}$  which can be attributed to decomposition of carbonates compounds formed.

**Figure 2(a)** shown FTIR spectra for the samples  $\text{LaMO}_3$  (Ni or Co), heated treated at  $220^\circ\text{C}$  and prepared by PQ method. Several bands were observed in such spectra with central point at  $1654\text{ cm}^{-1}$ ,  $1473\text{ cm}^{-1}$ ,  $866\text{ cm}^{-1}$  and  $600\text{ cm}^{-1}$  which can be attributed to the N-H, C=O, C-N, N-O and metal-O bonds [24,25]. The bands due EDTA vibrations still were observed in the calcined samples at  $700^\circ\text{C}$  (**Figure not shown**). Such results indicated that the temperature and time of calcinations were not sufficient for complete decomposition of residual material of the synthesis process.

FTIR spectra of  $\text{LaNi}_x\text{Co}_{1-x}\text{O}_3$  ( $0.4 \leq x \leq 0.6$ ;  $x = 1$ ) heated treated at  $300^\circ\text{C}$  and prepared by PP method showed bands between  $1643$ - $1538$  and at  $1410$ ,  $1249$ ,  $1067$  and  $642\text{ cm}^{-1}$  (**Figure 2(b)**). The bands observed at  $1643$ - $1538$  and  $1410\text{ cm}^{-1}$  were assigned to the asymmetric and symmetric carbonyl group stretching vibrations of ionized carboxylate. The bands at  $1249$  and  $1067\text{ cm}^{-1}$  could be attributed to nitrate ions. These bands were no longer observed as the materials were calcined at  $700^\circ\text{C}$ , suggesting the decomposition of the residual material of the synthesis process.

X-ray diffraction patterns of the precursor powders prepared by polymeric precursor and chelating precursor methods revealed the presence of amorphous structures. The formation of crystalline phases can be seen from the patterns of powders calcined at  $700^\circ\text{C}$  (**Figure 3**). For the

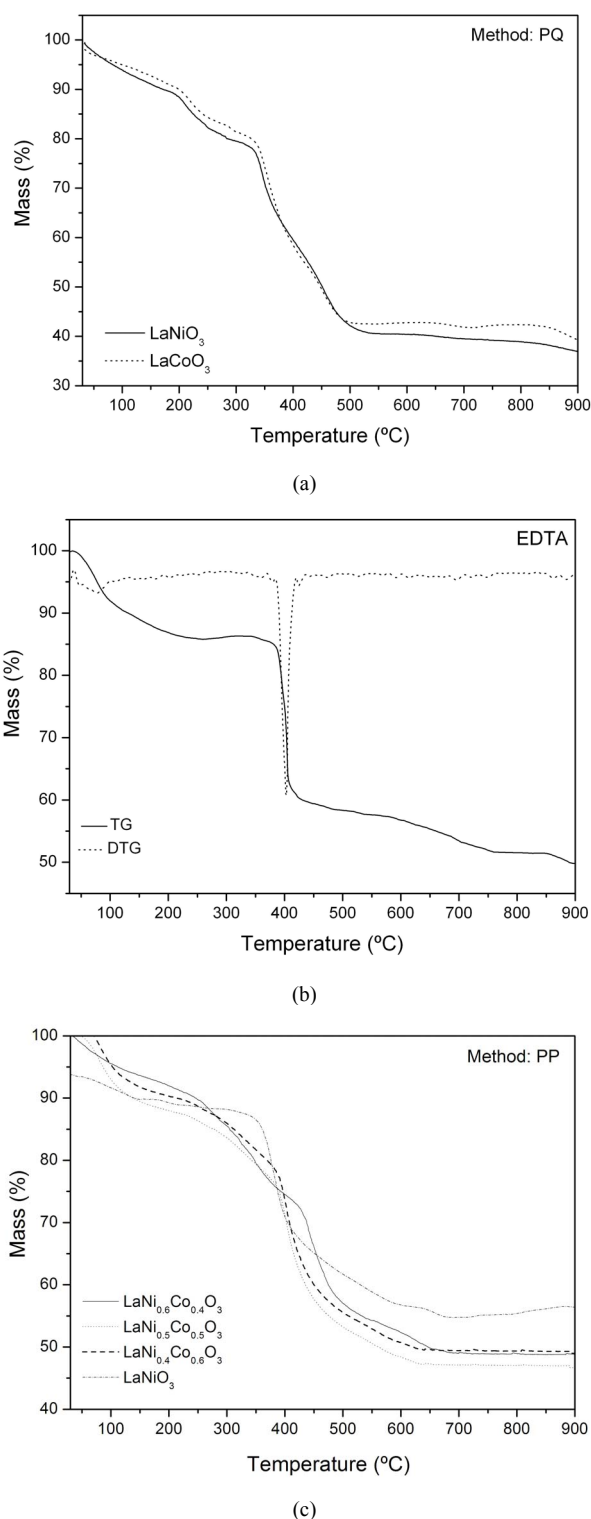
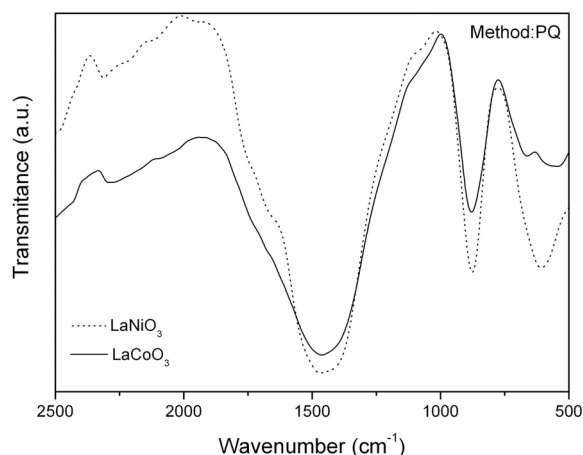
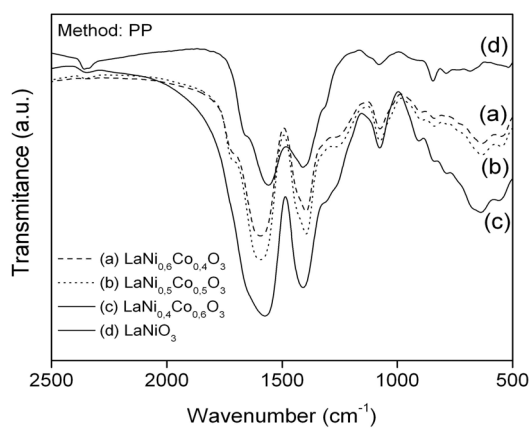


**Figure 1.** TG curves for (a)  $\text{LaMO}_3$  ( $M = \text{Ni}$  or  $\text{Co}$ ); (b) EDTA and (c)  $\text{LaNi}_x\text{Co}_{1-x}\text{O}_3$

samples  $\text{LaNi}_x\text{Co}_{1-x}\text{O}_3$  ( $0.4 \leq x \leq 0.6$ ;  $x = 1$ ) calcined at  $700^\circ\text{C}$  and prepared by PP method (**Figure 3(b)**), all the



(a)

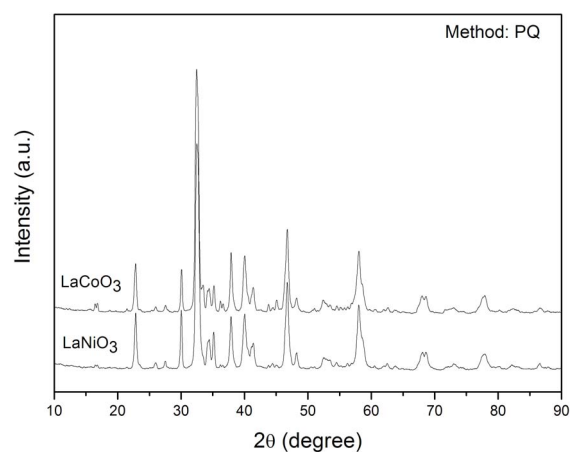


(b)

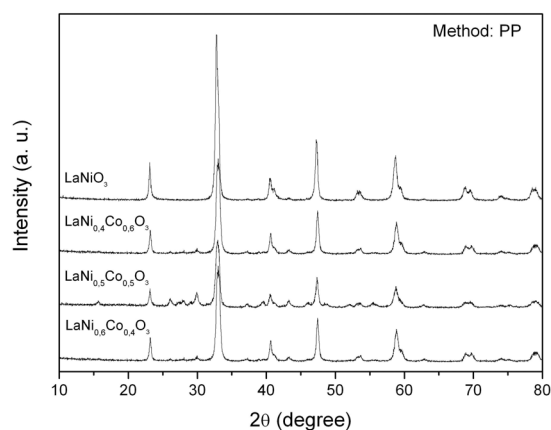
**Figure 2.** FTIR spectra for (a)  $\text{LaMO}_3$  ( $M = \text{Ni}$  or  $\text{Co}$ ) and (b)  $\text{LaNi}_x\text{Co}_{1-x}\text{O}_3$

samples consisted of single-phase materials exhibiting the perovskite structure, except for a minor phase observed on the  $\text{LaNi}_{0.5}\text{Co}_{0.5}\text{O}_3$  sample. The perovskite structure was characterized by rather intense peaks at  $2\theta = 33.1^\circ$ ,  $47.4^\circ$  and  $59.5^\circ$ . All perovskite peaks were attributed to rhombohedral unit cells, space group  $R3c$  (JCPDS 32-0296). According to XRD data, no significant changes occurred in the lattice parameters of the perovskite structure due to partial substitution of Ni for Co in its B sites. Such result was expected since the ionic radii of  $\text{Ni}^{3+}$  and  $\text{Co}^{3+}$  are rather similar. XRD also revealed that the structure of the resulting perovskite is similar to that of non-substituted lanthanum nickelate or cobalt perovskites [26-27]. Moreover, powders prepared by the polymeric precursor method depicted similar structure compared to the same powders prepared by other methods.

Well-resolved X-ray patterns were obtained for the samples  $\text{LaMO}_3$  (Ni or Co), calcined at  $700^\circ\text{C}$  and prepared by PQ method (**Figure 3(a)**) clearly suggesting the formation of a highly crystallized powder. For these samples, X-ray diffraction patterns showed peaks at  $2\theta =$



(a)



(b)

**Figure 3.** XRD patterns for (a)  $\text{LaMO}_3$  ( $M = \text{Ni}$  or  $\text{Co}$ ) and (b)  $\text{LaNi}_x\text{Co}_{1-x}\text{O}_3$

$32.4^\circ$ ,  $46.7^\circ$  and  $58.1^\circ$  which were attributed to perovskite structure [13]. All perovskite structure peaks identified were indexed as rhombohedral system. Peaks referent to carbonate sodium and sodium oxide also were observed suggesting that the crystallinity is not a function of the monophasic structure. Carbonate phase also was confirmed by FTIR and TG data. Therefore, the perovskite structure crystallizes from amorphous precursors and simultaneously occurs the formation of intermediate phase which can be decomposed at high temperatures. The  $\text{LaNi}_{0.5}\text{Co}_{0.5}\text{O}_3$  sample. The perovskite structure was characterized by rather intense peaks at  $2\theta = 33.1^\circ$ ,  $47.4^\circ$  and  $59.5^\circ$ . All perovskite peaks were attributed to rhombohedral unit cells, space group  $R3c$  (JCPDS 32-0296). According to XRD data, no significant changes occurred in the lattice parameters of the perovskite structure due to partial substitution of Ni for Co in its B sites. Such result was expected since the ionic radii of  $\text{Ni}^{3+}$  and  $\text{Co}^{3+}$  are rather similar. XRD also revealed that the structure of the

resulting perovskite is similar to that of non-substituted lanthanum nickelate or cobalt perovskites [26,27]. Moreover, powders prepared by the polymeric precursor method depicted similar structure compared to the same powders prepared by other methods.

Well-resolved X-ray patterns were obtained for the samples  $\text{LaMO}_3$  (Ni or Co), calcined at  $700^\circ\text{C}$  and prepared by PQ method (**Figure 3(a)**) clearly suggesting the formation of a highly crystallized powder. For these samples, X-ray diffraction patterns showed peaks at  $2\theta = 32.4^\circ$ ,  $46.7^\circ$  and  $58.1^\circ$  which were attributed to perovskite structure [13]. All perovskite structure peaks identified were indexed as rhombohedral system. Peaks referent to carbonate sodium and sodium oxide also were observed suggesting that the crystallinity is not a function of the monophasic structure. Carbonate phase also was confirmed by FTIR and TG data. Therefore, the perovskite structure crystallizes from amorphous precursors and simultaneously occurs the formation of intermediate phase which can be decomposed at high temperatures.

**Table 1** shows the results of the crystallite size of the perovskite phase. The crystallite size was calculated by the Scherrer laws. The crystallites are smaller when the perovskites are synthesized by PQ method when compared with the perovskite synthesized by PP method. In the **Table 1** also is shown the specific surface area values and average medium particle size for all the perovskites. For the samples  $\text{LaMO}_3$  (Ni or Co), calcined at  $700^\circ\text{C}$  and prepared by PQ method, the surface area were smaller than  $137\text{ m}^2/\text{g}$ . These values not are characteristics for the perovskite type oxides prepared by conventional synthesis method. This result is a consequence of the presence of carbonate phase showed in the XRD analysis. From the results showed in the **Table 1** also is possible to see that with the substitution of nickel by cobalt practically not provokes great changes in the surface area. Such result was expected since the ionic radii of  $\text{Ni}^{3+}$  and  $\text{Co}^{3+}$  are rather similar. The surface area for the samples  $\text{LaNi}_x\text{Co}_{1-x}\text{O}_3$  ( $0.4 \leq x \leq 0.6$ ;  $x = 1$ ) calcined at  $700^\circ\text{C}$  and prepared by PP method were lower than  $15\text{ m}^2/\text{g}$ . These values are characteristics for the perovskite type oxides prepared by polymeric precursor method and from the calcinations conditions used.

**Figure 4** shown SEM micrographs for all perovskites samples calcined at  $700^\circ\text{C}$  and prepared by PQ and PP

**Table 1. Specific surface area (SSA), average medium particle (Dm) and crystallite size (d) for the perovskites synthesized**

Samples/ Method	Dm ( $\mu\text{m}$ )	SSA ( $\text{m}^2/\text{g}$ )	d (nm)
$\text{LaNiO}_3$ , PQ	2.6	143.7	10.8
$\text{LaCoO}_3$ , PQ	2.7	132.1	9.5
$\text{LaNiO}_3$ , PP	21.4	28.7	12.9
$\text{LaNi}_{0.6}\text{Co}_{0.4}\text{O}_3$ , PP	39.6	12.2	16.2
$\text{LaNi}_{0.5}\text{Co}_{0.5}\text{O}_3$ , PP	38.4	12.7	14.7
$\text{LaNi}_{0.4}\text{Co}_{0.6}\text{O}_3$ , PP	41.3	11.5	14.1

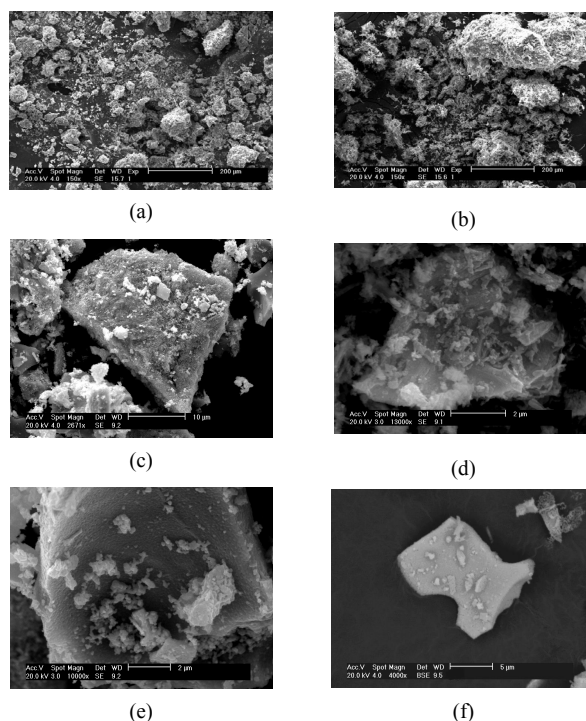


**Figure 4. SEM for (a)  $\text{LaNiO}_3$ , PQ; (b)  $\text{LaCoO}_3$ , PQ; (c)  $\text{LaNi}_{0.6}\text{Co}_{0.4}\text{O}_3$ , PP; (d)  $\text{LaNi}_{0.5}\text{Co}_{0.5}\text{O}_3$ , PP; (e)  $\text{LaNi}_{0.4}\text{Co}_{0.6}\text{O}_3$ , PP; and (f)  $\text{LaNiO}_3$ , PP**

methods. SEM micrographs showed non-uniform particles with sizes ranging from 2 to  $20\text{ }\mu\text{m}$ . Such distribution in particle size may be attributed to the preparation method and calcination temperature range used. The perovskites prepared by PQ and PP methods showed similar non-uniform particles when were compared to the same powders prepared by other methods.

#### 4. Conclusions

This work was carried out to investigate the effect of the preparation methods in the perovskite structure formation. The effect of partial substitution of Ni for Co in the B sites of  $\text{LaNiO}_3$  perovskites on the structural, morphological and surface properties also was studied. In accordance with TG curves and FTIR spectra, all organic residual material of the synthesis process decomposed up to  $650^\circ\text{C}$  for the precursor powders synthesized by polymeric precursor method. For the other hand, for the precursor powders prepared by chelating precursor method, all organic residual material of the synthesis process also decomposed up to  $650^\circ\text{C}$ , but in this case the decompositions lead to the formation of secondary phase in this temperature.

X-ray diffraction patterns revealed the formation of the rhombohedral perovskite structure in all samples prepared by both synthesis method and after calcinations at  $700^\circ\text{C}$ . The results showed that the preparation method resulted in oxides with the intended structure. Minor phases attrib-

uted to impurities were observed in the  $\text{LaNi}_{0.5}\text{Co}_{0.5}\text{O}_3$  prepared by polymeric precursor method and in all the samples prepared by chelating precursor method, which was attributed to carbonate phase.

In the perovskites prepared by PP method, the replacement of Ni by Co did not cause significant changes in the lattice parameters. The perovskites prepared by PP method are characterized by relatively wide particle size distributions with particles ranging from 2 to 20  $\mu\text{m}$  and specific surface area about 15  $\text{m}^2/\text{g}$ . The perovskites prepared by PQ method showed similar structure compared to the same powders prepared by other methods, having advantage strength how a little particle size and surface area higher 100  $\text{m}^2/\text{g}$ .

## 5. Acknowledgements

The authors would like to thank CNPq/Projeto n°550244/2007-7 and UFS/Edital PAIRD 2008 for the financial support of this study.

## REFERENCES

- [1] T.-R. Ling, Z.-B. Chen and M.-D. Lee, "Studies on Catalytic and Conductive Properties of  $\text{LaNiO}_3$  for Oxidation of  $\text{C}_2\text{H}_5\text{OH}$ ,  $\text{CHO}$  and  $\text{CH}_4$ ," *Catalysis Today*, Vol. 26, No. 1, 1995, pp. 79-86.
- [2] T. Hirohisa and M. Makoto, "Advances in Designing Perovskite Catalysts," *Current Opinion in Solid State and Materials Science*, Vol. 5, No. 5, 2001, pp. 381-387.
- [3] S. Liu, K. Li and R. Hughes, "Preparation of  $\text{SrCe}_{0.95}\text{Yb}_{0.05}\text{O}_{3-\alpha}$  Perovskite for Use as a Membrane Material in Hollow Fibre Fabrication," *Materials Research Bulletin*, Vol. 39, No. 1, 2004, pp. 119-133.
- [4] A. M. G. Pedrosa, J. D. G. Fernandes, D. M. Melo, A. S. Araújo, M. J. B. Souza and D. K. Gomes, "Synthesis and Catalytic Properties of Lanthanum Nickelate Perovskite Materials," *Reaction Kinetics and Catalysis Letters*, Vol. 84, No. 1, 2005, pp. 3-9.
- [5] E. Campagnoli, A. Tavares, L. Fabbrini, I. Rossetti, Y. A. Dubitsky, A. Zaopo and L. Forni, "Effect of Preparation Method on Activity and Stability of  $\text{LaMnO}_3$  and  $\text{LaCoO}_3$  Catalysts for the Flameless Combustion of Methane," *Applied Catalysis B: Environmental*, Vol. 55, No. 2, 2005, pp. 133-139.
- [6] S. Liu, X. Tan, K. Li, R. Hughes, "Synthesis of Strontium Cerates-Based Perovskite Ceramics via Water-Soluble Complex Precursor Routes," *Ceramics International*, Vol. 28, No. 3, 2002, pp. 327-335.
- [7] A. A. Leontiou, A. K. Ladavos and P. J. Pomonis, "Catalytic NO Reduction with CO on  $\text{La}_{1-x}\text{Sr}_x(\text{Fe}^{3+}/\text{Fe}^{4+})\text{O}_{3\pm\delta}$  Perovskite-Type Mixed Oxides ( $x = 0.00, 0.15, 0.30, 0.40, 0.60, 0.70, 0.80,$  and  $0.90$ )," *Applied Catalysis A: General*, Vol. 241, No. 1-2, 2003, pp. 133-141.
- [8] H. Tanaka and M. Misono, "Advances in Designing Perovskite Catalysts," *Current Opinion in Solid State and Materials Science*, Vol. 5, No. 5, 2001, pp. 381-387.
- [9] N. Yamazoe and Y. Teraoka, "Oxidation Catalysis of Perovskites: Relationships to Bulk Structure and Composition (Valency, Defect, etc.)," *Catalysis Today*, Vol. 8, No. 2-3, 1990, pp. 175-199.
- [10] K. Kleveland, M. A. Einarsrud and T. Grande, "Sintering of  $\text{LaCoO}_3$  Based Ceramics," *Journal of European Ceramic Society*, Vol. 20, No. 2, 2000, pp. 185-193.
- [11] D. Klvana, J. Vaillancourt, J. Kirchnerova and J. Chaouki, "Combustion of Methane over  $\text{La}_{0.66}\text{Sr}_{0.34}\text{Ni}_{0.3}\text{Co}_{0.7}\text{O}_3$  and  $\text{La}_{0.4}\text{Sr}_{0.6}\text{Fe}_{0.4}\text{Co}_{0.6}\text{O}_3$  Prepared by Freeze-Drying," *Applied Catalysis A: General*, Vol. 109, No. 2-3, 1994, pp. 181-193.
- [12] N. Gunasekaran, S. Saddawi and J. J. Carberry, "Effect of Surface Area on the Oxidation of Methane over Solid Oxide Solution Catalyst  $\text{La}_{0.8}\text{Sr}_{0.2}\text{MnO}_3$ ," *Journal of Catalysis*, Vol. 159, No. 1, 1996, pp. 107-111.
- [13] M. Alifanti, R. Auer, J. Kirchnerova, F. Thyron, P. Grange and B. Delmona, "Activity in Methane Combustion and Sensitivity to Sulfur Poisoning of  $\text{La}_{1-x}\text{Ce}_x\text{Mn}_{1-y}\text{Co}_y\text{O}_3$  Perovskite Oxides," *Applied Catalysis B: Environmental*, Vol. 41, No. 1-2, 2003, pp. 71-81.
- [14] T. Nitadori and M. Misono, "Catalytic Properties of  $\text{La}_{1-x}\text{A}'_x\text{FeO}_3$  ( $\text{A}' = \text{Sr}, \text{Ce}$ ) and  $\text{La}_{1-x}\text{Ce}_x\text{CoO}_3$ ," *Journal of Catalysis*, Vol. 93, No. 2, 1985, pp. 459-466.
- [15] A. K. Azada, S.-G. Eriksson, S. A. Ivanov, R. Mathieu, P. Svedlindh, J. Eriksen and H. Rundlöf, "Synthesis, Structural and Magnetic Characterisation of the Double Perovskite  $\text{A}_2\text{MnMoO}_6$  ( $\text{A} = \text{Ba}, \text{Sr}$ )," *Journal of Alloys and Compounds*, Vol. 364, No. 1-2, 2004, pp. 77-82.
- [16] F.-C. Buciuman, F. Patcas, J.-C. Menezes, J. Barbier, T. Hahn and H.-G. Lintz, "Catalytic Properties of  $\text{La}_{0.8}\text{A}_{0.2}\text{MnO}_3$  ( $\text{A} = \text{Sr}, \text{Ba}, \text{K}, \text{Cs}$ ) and  $\text{LaMn}_{0.8}\text{B}_{0.2}\text{O}_3$  ( $\text{B} = \text{Ni}, \text{Zn}, \text{Cu}$ ) Perovskites: 1. Oxidation of Hydrogen and Propene," *Applied Catalysis Bi Environmental*, Vol. 35, No. 3, 2002, pp. 175-183.
- [17] R. Spinicci, A. Tofanari, M. Faticanti, I. Pettiti and P. Porta, "Hexane Total Oxidation on  $\text{LaMO}_3$  ( $\text{M} = \text{Mn}, \text{Co}, \text{Fe}$ ) Perovskite-Type Oxides," *Journal of Molecular Catalysis A: Chemical*, Vol. 176, No. 1-2, 2001, pp. 247-252.
- [18] G. Saracco, F. Geobaldo and G. Baldi, "Methane Combustion on Mg-Doped  $\text{LaMnO}_3$  Perovskite Catalysts," *Applied Catalysis B: Environmental*, Vol. 20, No. 4, 1999, pp. 277-288.
- [19] R. Zenati, C. Bernard, C. Calmet, S. Guillemet, G. Fantozzi and B. Durand, "Internal Friction Investigation of Phase Transformation in nearly Stoichiometric  $\text{LaMnO}_{3\pm\delta}$ ," *Journal of the European Ceramic Society*, Vol. 25, No. 6, 2005, pp. 935-941.
- [20] M. D. S. Kumar, T. M. Srinivasan, P. Ramasamy and C. Subramanian, "Synthesis of Lanthanum Aluminate by a Citrate-Combustion Route," *Materials Letters*, Vol. 25, No. 3-4, 1995, pp. 171-174.
- [21] L. Hong, F. Guo and J. Lin, "From Chelating Precursors to  $\text{La}_{0.05}\text{Sr}_{0.95}\text{CoO}_{3-y}$  Oxide," *Materials Research Bulletin*, Vol. 34, No. 12-13, 1999, pp. 1943-1958.
- [22] A. M. G. Pedrosa, M. J. B. Souza, B. A. Marinkovic, D. M. A. Melo and A. S. Araújo, "Structure and Properties of Bifunctional Catalysts Based on Zirconia Modified by

- Tungsten Oxide Obtained by Polymeric Precursor Method,” *Applied Catalysis A: General*, Vol. 342, No. 1-2, 2008, pp. 56-62.
- [23] A. M. G. Pedrosa, D. M. A. Melo, M. J. B. Souza, A. O. S. Silva and A. S. Araujo, “Effect of Cerium, Holmium and Samarium Ions on the Thermal and Structural Properties of the HZSM-12 Zeolite,” *Journal of Thermal Analysis and Calorimetry*, Vol. 84, No. 2, 2006, pp. 503-509.
- [24] D. Zhou, G. Huang, X. Chen, J. Xu and S. Gong, “Synthesis of  $\text{LaAlO}_3$  via Ethylenediaminetetraacetic Acid Precursor,” *Materials Chemistry and Physics*, Vol. 84, No. 1, 2004, pp. 33-36.
- [25] Y. H. Huang, Z.-G. Xu, C.-H. Yan, Z.-M. Wang, T. Zu, C.-S. Liao, S. Gao and G.-X. Xu, “Soft Chemical Synthesis and Transport Properties of  $\text{La}_{0.7}\text{Sr}_{0.3}\text{MnO}_3$  Granular Perovskites,” *Solid State Communications*, Vol. 114, No. 1, 2000, pp. 43-47.
- [26] M. Popa and M. Kakihana, “Synthesis of Lanthanum Cobaltite ( $\text{LaCoO}_3$ ) by the Polymerizable Complex Route,” *Solid State Ionics*, Vol. 151, No. 1-4, 2002, pp. 251-257.
- [27] S. Nakayama, M. Okazaki, Y. L. Aung and M. Sakamoto, “Preparations of Perovskite-Type Oxides  $\text{LaCoO}_3$  from Three Different Methods and their Evaluation by Homogeneity, Sinterability and Conductivity,” *Solid State Ionics*, Vol. 158, No. 1-2, 2003, pp. 133-139.